2844 *Inorg. Chem.* **2010**, *49*, 2844–2850
DOI: 10.1021/ic902247w

Inorganic Chemistry
Article

Gas-Phase Thermolysis of a Guanidinate Precursor of Copper Studied by Matrix Isolation, Time-of-Flight Mass Spectrometry, and Computational Chemistry

Jason P. Coyle,[†,‡] Paul A. Johnson,[‡,§] Gino A. DiLabio,[§] Seán T. Barry,[*,‡] and Jens Müller[*,†]

[†]*Department of Chemistry, University of Saskatchewan, 110 Science Place, Saskatoon, Saskatchewan, S7N 5C9 Canada,* [‡]*Department of Chemistry, Carleton University, 1125 Colonel By Drive, Ottawa, Ontario, K1S 5B6 Canada, and* [§]*National Institute for Nanotechnology, National Research Council of Canada, 11421 Saskatchewan Drive, Edmonton, Alberta, Canada T6G 2M9*

Received November 13, 2009

The fragmentation of the copper(I) guanidinate $[Me_2NC(N\textit{i}Pr)_2Cu]_2$ (**1**) has been investigated with time-of-flight mass spectrometry (TOF MS), matrix-isolation FTIR spectroscopy (MI FTIR spectroscopy), and density functional theory (DFT) calculations. Gas-phase thermolyses of **1** were preformed in the temperature range of 100−800 °C. TOF MS and MI FTIR gave consistent results, showing that precursor **1** starts to fragment at oven temperatures above 150 °C, with a close to complete fragmentation at 260 °C. Precursor **1** thermally fragments to $Cu_{(s)}$, H_2(g), and the oxidized guanidine $Me_2NC(=N\textit{i}Pr)(N=CMe_2)$ (**3**). In TOF MS experiment, **3** was clearly indentified by its molecular ion at 169.2 u. Whereas H_2^+ was detected, atomic Cu was not found in gas-phase thermolysis. In addition, the guanidine $Me_2NC(N\textit{i}Pr)(NH\textit{i}Pr)$ (**2**) was detected as a minor component among the thermolysis products. MI thermolysis experiments with precursor **1** were performed, and species evolving from the thermolysis oven were trapped in solid argon at 20 K. These species were characterized by FTIR spectroscopy. The most indicative feature of the resulting spectra from thermolysis above 150 °C was a set of intense and structured peaks between 1600 and 1700 cm^{-1}, an area where precursor **1** does not have any absorbances. The guanidine **2** was matrix-isolated, and a comparison of its FTIR spectrum with the spectra of the thermolysis of **1** indicated that species **2** was among the thermolysis products. However, the main IR bands in the range of 1600 and 1700 cm^{-1} appeared at 1687.9, 1668.9, 1635.1, and 1626.6 cm^{-1} and were not caused by species **2**. The oxidized guanidine **3** was synthesized for the first time and characterized by ^{1}H NMR and FTIR spectroscopy. A comparison of an FTIR spectrum of matrix isolated **3** with spectra of the thermolysis of **1** revealed that the main IR bands in the range of 1600 and 1700 cm−1 are due to the presence of **3**. The isomers exhibit the NMe_2 group *cis* or *trans* to the *i*Pr group, with *cis*-**3** being significantly less stable than *trans*-**3**. At higher temperature secondary thermal fragments had been observed. For example at 700 °C, TOF MS and MI FTIR data showed that species **2** and **3** both eliminate $HNMe_2$ to give the carbodiimides *i*PrNCN*i*Pr (CDI) and *i*PrNCN[C(=CH_2)Me] (**4**), respectively. A DFT study of the decomposition of compound **1** was undertaken at the B3LYP/6-31+G(d,p) level of theory employing dispersion-correcting potentials (DCPs). The DFT study rationalized both carbodiimide deinsertion and β-hydrogen elimination as exergonic decomposition pathways (ΔG = −44.4 kcal/mol in both cases), but experiment showed β-hydrogen elimination to be the favorable route.

Introduction

Thin films of copper metal are of utmost interest in microelectronics, specifically for use as an interconnect material. Several copper(I) precursors have been reported for chemical vapor deposition (CVD) and atomic layer deposition (ALD), including β-diketonates,[1−4] β-diketiminates,[5] amidinates,[6−9] and guanidinates.[10]

*To whom correspondence should be addressed. E-mail: sbarry@connect.carleton.ca (S.T.B.), jens.mueller@usask.ca (J.M.).

(1) Chen, T. Y.; Omnes, L.; Vaisserman, J.; Doppelt, P. *Inorg. Chim. Acta* **2004**, *357*, 1299–1302.
(2) Bollmann, D.; Merkel, R.; Klumpp, A. *Microelectron. Eng.* **1997**, *37-8*, 105–110.
(3) Lagalante, A. F.; Hansen, B. N.; Bruno, T. J.; Sievers, R. E. *Inorg. Chem.* **1995**, *34*, 5781–5785.
(4) Wenzel, T. J.; Williams, E. J.; Haltiwanger, R. C.; Sievers, R. E. *Polyhedron* **1985**, *4*, 369–378.
(5) Park, K. H.; Marshall, W. J. *J. Am. Chem. Soc.* **2005**, *127*, 9330–9331.
(6) Li, Z. W.; Rahtu, A.; Gordon, R. G. *J. Electrochem. Soc.* **2006**, *153*, C787–C794.
(7) Li, Z. W.; Barry, S. T.; Gordon, R. G. *Inorg. Chem.* **2005**, *44*, 1728–1735.
(8) Lim, B. S.; Rahtu, A.; Gordon, R. G. *Nat. Mater.* **2003**, *2*, 749–754.
(9) Lim, B. S.; Rahtu, A.; Park, J. S.; Gordon, R. G. *Inorg. Chem.* **2003**, *42*, 7951–7958.
(10) Coyle, J. P.; Monillas, W. H.; Yap, G. P. A.; Barry, S. T. *Inorg. Chem.* **2008**, *47*, 683–689.

Published on Web 02/12/2010

Scheme 1

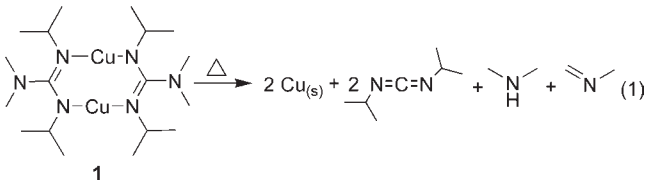

1

The guanidinate dimer of copper(I), $[Me_2NC(NiPr)_2Cu]_2$ (**1**), deposits copper in a CVD process above 225 °C as a nanocrystalline film;[10] similar reactivity is known for the acetamidinatocopper(I) dimer.[9] An interesting aspect of the deposition is that these precursors act as *single source* precursors for copper, meaning that they do not require a second, reducing precursor to produce copper metal. The solution-phase thermolysis of the guanidinate compound **1** showed the production of diisopropylcarbodiimide (CDI), and thus we suggested a mechanism whereby CDI deinserted from the ligand to produce a copper amide intermediate, $Cu_2(NMe_2)_2$, which then eliminated an imine and an amine to produce metallic copper (Scheme 1).[10]

We wanted to further investigate this mechanism, particularly in light of a recent report of β-hydrogen elimination as a potential thermolysis route.[11] In addition, we recently unraveled the fragmentation of an alumina ALD precursor, the aluminum guanidinate $[Me_2NC(NiPr)_2]Al(NMe_2)_2$, by time-of-flight mass spectrometry (TOF MS) and matrix-isolation FTIR spectroscopy (MI FTIR spectroscopy).[12] Using these techniques, we have shown that this precursor eliminates CDI to give the monomeric aluminum amide $Al(NMe_2)_3$ above 300 °C.[12] Thus, we employed these techniques to further investigate the gas-phase thermolyses of the copper precursor **1** in the temperature range of 100−800 °C. We report on results of TOF MS, MI FTIR spectroscopy, and DFT calculations.

Results and Discussions

Since Pimentel's pioneering work on matrix-isolation spectroscopy,[13,14] this technique matured into a well-known method to trap and identify reactive intermediates. Mass spectrometry is a highly sensitive method to investigate gas-phase species, and it has been used to elucidate thermal fragmentations of precursors. Recently, we combined both techniques in a unique apparatus in which the thermolysis of a CVD precursor can be investigated using MI FTIR spectroscopy and TOF MS.[12] The facility was designed in such a way that a series of experiments can be performed using one method, which can then be followed by a similar series of experiments on the same precursor sample and carrier gas supply using the second method. Consequently, MI FTIR and TOF MS data are collected consecutively, but the conditions in both series of experiments are kept as similar as possible so that their data complement one another.

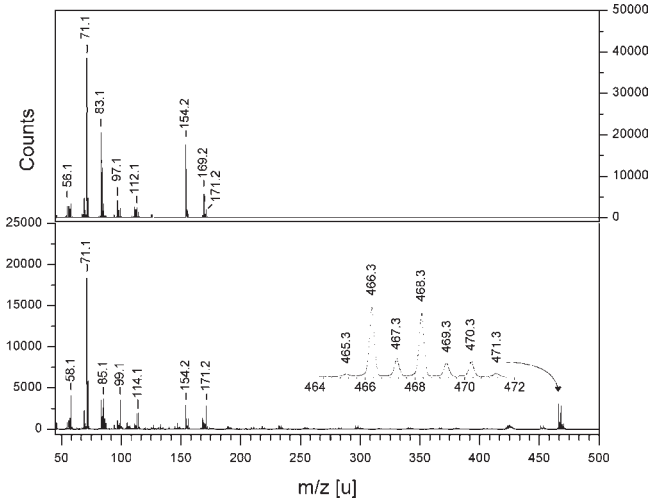

Figure 1. Overview MS of the copper guanidinate **1** with thermolysis oven at 130 °C (no thermal fragmentation; bottom spectrum; M^+ of **1** enlarged) and at 260 °C (complete thermal fragmentation of **1**; top spectrum).

Chart 1. Protonated and Oxidized Ligand with Calculated Masses

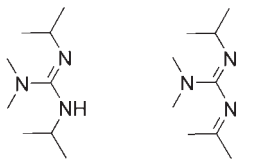

2 (171.17 u) **3** (169.16 u)

TOF MS. The mass spectrum at the bottom of Figure 1 shows the typical ion pattern of precursor **1** in the absence of any thermal decomposition; all fragments of the molecular ion were caused by ion impact ionization at 70 eV of the precursor **1**. An oven temperature of 130 °C was used to avoid any build-up of **1** in the apparatus through condensation. The highest detectable masses in this spectrum are due to M^+ of **1** (enlargement in Figure 1); its isotopic pattern agrees well with the calculated one (see Experimental Section). It should be noted that the ion at 465.3 u is not part of the isotopic pattern of $\mathbf{1}^+$, but results from the loss of one H atom ($\mathbf{1}^+ - H$). When the oven temperature was increased to 260 °C (Figure 1 top spectrum), $\mathbf{1}^+$ could no longer be detected,[15] and the highest mass appeared at 171.2 u followed by a mass of higher intensity at 169.2 u. The mass of 171.2 u matches with the empirical formula of $C_9H_{21}N_3^+$ (calc. mass of 171.17 u) and can be interpreted as the cation of the protonated ligand **2** (Chart 1). The peak at 169.2 u fits well to $C_9H_{19}N_3^+$ (calc. mass of 169.16 u) and can be interpreted as dehydrogenated **2**. From the numerous possibilities to assign a structural formula to the mass of 169.2 u, we assign structure **3** (Chart 1) for reasons that will become apparent in the following discussion.

Figure 2 shows how signal intensities of selected ions changed in the temperature range of 130−200 °C. The signal intensity of M^+ (466.3 u) of the precursor **1** decreases slightly from 160 to 170 °C, followed by a steeper decrease at temperatures above 170 °C. A comparable change of

(11) Wu, J. P.; Li, J. Y.; Zhou, C. G.; Lei, X. J.; Gaffney, T.; Norman, J. A. T.; Li, Z. W.; Gordon, R.; Cheng, H. S. *Organometallics* **2007**, *26*, 2803–2805.
(12) Ziffle, L. C.; Kenney, A. P.; Barry, S. T.; Müller, J. *Polyhedron* **2008**, *27*, 1832–1840.
(13) Whittle, E.; Dows, D. A.; Pimentel, G. C. *J. Chem. Phys.* **1954**, *22*, 1943.
(14) Norman, I.; Pimentel, G. C. *Nature* **1954**, *174*, 508–509.

(15) Only traces of $\mathbf{1}^+$ were detectable; intensity of 466.3 u was 25 counts out of 10 million sweeps.

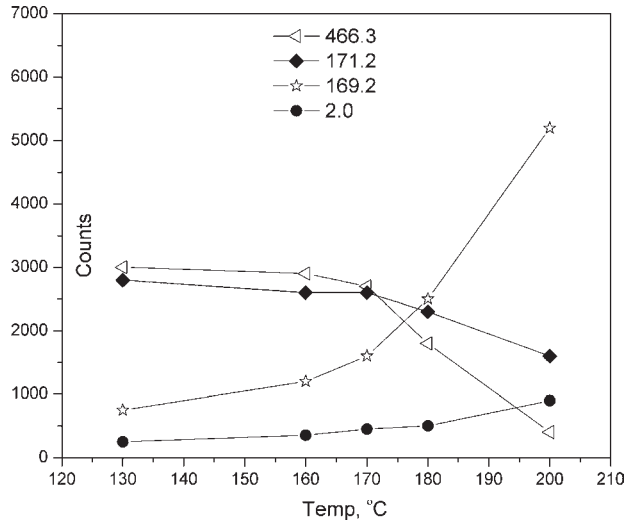

Figure 2. Temperature dependence of intensities of selected ions arising from the thermolysis of **1** [m/z = 466.3 ($\mathbf{1}^+$), 171.2 ($\mathbf{2}^+$), 169.2 ($\mathbf{3}^+$), 2.0 (H_2^+) u].

Scheme 2

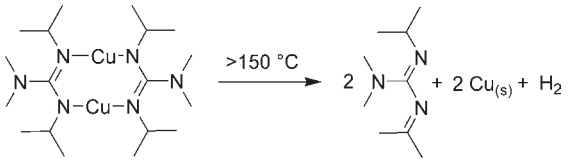

1 **3**

intensities was observed for the signal of $\mathbf{2}^+$ (171.2 u). At the same time, the signal of $\mathbf{3}^+$ (169.2 u) showed a significant increase in intensity, which indicates that $\mathbf{3}^+$ is an ion of a thermolysis fragment of precursor **1**.

In addition to the identification of the peak at 169.2 u, which we assign to the structural formula **3** (Chart 1), there is a significant increase of the signal intensity at 2.0 u, which is due to the presence of H_2^+. Copper atoms were not detected in the gas phase; however, after a long series of thermolyses, the thermolysis oven was inspected and had a copper color at the oven orifice. This is not surprising, as it was shown that **1** is a precursor for the thermal deposition of Cu.[10] On the basis of these data, we propose that the thermolysis of precursor **1** can be described as shown in Scheme 2. We performed DFT calculations at the B3LYP/6-31+G(d,p) level of theory employing dispersion-correcting potentials (DCPs), which showed that the production of **3** through β-hydrogen elimination is thermodynamically favorable (ΔG = −44.4 kcal/mol).[16]

Compound **3** is the formal dehydrogenated product of the protonated ligand **2**, and it is feasible that **2**, instead of **3**, is the primary thermolysis product of the precursor **1**. Species **2** could further decompose to give the detected species **3**. Therefore, an independent thermolysis series with the protonated ligand **2** as a starting compound was undertaken. This study revealed that, for temperatures of up to 800 °C in the presence of a copper metal surface, species **2** does not eliminate H_2 to give **3**. In all mass spectra of **2** the signal at 169.2 u appeared only with negligible intensities compared to that at 171.2 u ($\mathbf{2}^+$).

When considering Scheme 2, it might seem possible for the reaction to proceed by disproportion of Cu(I) to Cu(II) and Cu(0), giving an undetected (and perhaps unstable and transient) copper(II) species. This has been suggested for the amidinate depositing copper on silicon dioxide.[17] However, our DFT calculations (at the B3LYP/6-31+G(d,p) level of theory with DCPs and making the same assumptions as previous) show this to be unlikely for a gas phase species: it would have a ΔG of 10.9 kcal/mol (compared to −44.4 kcal/mol for β-hydrogen elimination from a copper(I) species). As well, the FTIR spectra throughout the series of thermolysis experiments did not show any peaks that could not be assigned specifically to the reactants and products of Scheme 2. Specifically, the region from 1500−1800 cm^{-1} (where a C=N stretching mode for a Cu(II) guanidinate species would appear) contained no unassigned peaks. Finally, similar mechanistic work for surface-bound copper species on a nickel surface resulting from the thermolysis of a copper amidinate similarly found no experimental evidence for a copper(II) species.[18] The sum of the evidence suggests that we do not see a copper(II) species in these experiments.

Considering Scheme 2, it also seems possible that the decomposition might proceed by a process involving homolytic scission of the Cu−N bonds to produce free radical intermediates, which may then disproportionate to form **2** and **3**. DFT calculations at the B3LYP/6-31+G(d,p) level of theory with DCPs indicate that this process is endergonic by 33.6 kcal/mol, and therefore also unlikely. The thermolysis of copper(I) alkyls has been studied by Whitesides et al.[19−21] Their study of *n*-butylcopper(I) compounds revealed a β-hydride elimination pathway.[19] The decomposition of 1-propenylcopper(I) was also found not to proceed by a pathway involving free radical intermediates despite the stability of the vinyl radical.[20] However, neophyl(tri-*n*-butylphosphine)copper(I) was found to produce the neophyl radical, which is known to rearrange to an exceptionally stable radical.[21] These studies have shown that free radicals are unlikely intermediates in the thermolysis of copper(I) alkyls unless the free radical itself is very stable. Copper(I) amides have been found to decompose via β-hydride elimination and to be more stable than their corresponding alkyls.[22] On this basis, it seems unlikely that a mechanism involving free radical intermediates is involved in the decomposition of **1**.

Alternatively, one might expect the thermolysis reaction as illustrated in Scheme 2 to be initiated by the

(16) This value was calculated using ΔG = −127.3 kcal/mol for the process $2Cu_{(g)} \rightarrow 2Cu_{(s)}$ calculated from data tabulated in: Lide, D. R. *Handbook of Chemistry and Physics* 79th ed.; CRC Press: Boca Raton, FL, 1998. Using the same level of theory, ΔG is computed to be −11.5 kcal/mol for the CDI deinsertion process shown in Scheme 1.

(17) Dai, M.; Kwon, J.; Halls, M. D.; Gordon, R. G.; Chabal, Y. J. *Langmuir* **2010**, ASAP, DOI: 10.1021/la903212c.
(18) Qiang Ma, Q.; Hansheng Guo, G.; Gordon, R. G.; Francisco Zaera, F. *Chem. Mater*. **2010**, *22*, 352–359.
(19) Whitesides, G. M.; Stedronsky, E. R.; Casey, C. P.; San Filippo, J. *J. Am. Chem. Soc*. **2002**, *92*, 1426–1427.
(20) Whitesides, G. M.; Casey, C. P.; Krieger, J. K. *J. Am. Chem. Soc*. **2002**, *93*, 1379–1389.
(21) Whitesides, G. M.; Panek, E. J.; Stedronsky, E. R. *J. Am. Chem. Soc*. **2002**, *94*, 232–239.
(22) Tsuda, T.; Watanabe, K.; Miyata, K.; Yamamoto, H.; Saegusa, T. *Inorg. Chem*. **1981**, *20*, 2728–2730.

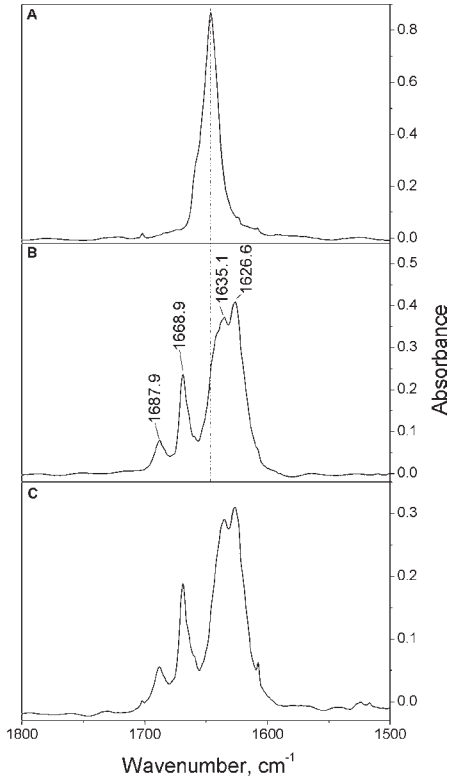

Figure 3. Measured IR spectra of copper guanidinate **1** and its thermolysis products (*x* axis, 1500−1800 cm^{-1}; *y* axis, absorbance). Spectrum A: **2** in solid argon (thermolysis oven at 260 °C); see Supporting Information, Figure S3 for a complete IR spectrum. Spectrum B: results of a thermolysis of complex **1** at 260 °C; see Supporting Information, Figure S2 for a complete IR spectrum. Spectrum C: **3** in solid argon (thermolysis oven at 260 °C); residual amounts of **2** have been electronically eliminated; see Supporting Information, Figure S4 for a complete IR spectrum.

decomposition of the dimer **1** to form two copper guanidinate monomers, which subsequently decompose. Using DFT calculations, we predict that this pathway is very unlikely, namely, ΔG = 66.7 kcal/mol for the formation of two copper(I) guanidinate monomers. In addition, there was no evidence of the monomer [$Me_2NC(NiPr)_2Cu$] in the thermolysis series of the dimer **1**; the measured intensities of signals showing fragments with one Cu atom indicated that they were caused by the impact ionization of **1** alone.

MI FTIR Spectroscopy. The thermal decomposition of precursor **1** was also investigated with MI FTIR spectroscopy, using similar experimental conditions as for the TOF MS experiments discussed above. At oven temperatures of up to 150 °C, IR spectra did not change, thus indicating that precursor **1** did not decompose (see Supporting Information, Figure S1). At temperatures of 160 °C, new IR peaks indicated the onset of the thermolysis. The most indicative feature of the resulting spectrum was a set of intense and structured peaks between 1600 and 1700 cm^{-1}, an area where precursor **1** does not have any absorbances. Spectrum B of Figure 3 shows the result of a thermolysis of **1** at 260 °C. The investigation of **1** by TOF MS revealed that the protonated ligand **2** was a product in the gas phase. To find out if **2** was also present in the matrixes, a MI FTIR spectrum of the synthesized sample of **2** was measured (Figure 3, spectrum A). The comparison of spectrum A with B indicates that **2** was one of the thermolysis products of **1**. Species **2** has its most intense IR band at 1646.0 cm^{-1}, which appears as a shoulder of the intense features between 1600 and 1700 cm^{-1} in spectrum B (see dotted line in Figure 3). The TOF MS experiments clearly indicated that **3** was one of the key fragments of the thermolysis of the copper precursor **1** (Scheme 2). Similarly to the identification of **2** as a thermolysis product, we intended to identify **3** through comparison with FTIR spectra. To our surprise, species **3** was unknown in the literature, and consequently needed to be synthesized.

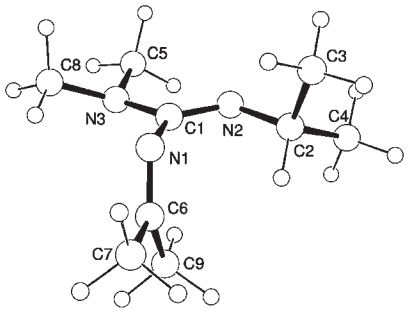

trans-**3**

Figure 4. Optimized structure for *trans*-**3** obtained with B3LYP/6-31+G(d,p)-DCP.

On the basis of a known method to synthesize imines from secondary amines,[23] **2** was oxidized using 2 equiv of $CuBr_2$ and 2 equiv of $LiOtBu$ to give species **3**. Species **3** was first characterized by ^1H NMR spectroscopy, which showed that in addition to the target compound **3**, small amounts of the starting compound **2** were present. In particular, the two singlets of equal intensity at 1.43 and 1.72 ppm (in C_6D_6) clearly revealed the two diastereotopic Me groups of the N=CMe_2 moiety of **3** (Chart 1). This compound proved very difficult to isolate from the parent guanidine and ^{t}BuOH, all of which have very similar boiling points, but the IR was captured in matrix isolation, and matched the calculated vibrational frequencies such that we are satisfied of its formulation (Supporting Information, Figure S4, Table S1). We are continuing to try to isolate this material to further our thermolysis studies of this system.

A so-prepared sample was vaporized and trapped in solid argon; spectrum C of Figure 3 shows the resulting IR spectrum. All measured IR bands of **3** (spectrum C) are present in spectra of the thermolysis of precursor **1** (spectrum B), giving strong evidence that **3** is a thermolysis product. The structured IR band in the range of 1600 and 1700 cm^{-1} with four maxima at 1687.9, 1668.9, 1635.1, and 1626.6 cm^{-1} must be caused by C=N stretching modes. As compound **3** exhibits two C=N bonds, two C=N stretching modes are expected in the IR range. The fact that the IR absorbance between 1600 and 1700 cm^{-1} shows more than two bands, suggests that perhaps different isomers of **3** are present. To better understand the structure of the IR band in the C=N stretching region, DFT calculations at the BLYP/6-31G(d) level of theory were performed. The lowest energy structure of **3** (Figure 4) has a *trans* orientation of the Me_2N and the *i*Pr group, and was the only isomer that appeared in an appreciable amount (Figure 4).

The calculated frequencies of the C=N stretches of *trans*-**3** fit very well to the experimental data: the calculated

(23) Yamaguchi, J.; Takeda, T. *Chem. Lett.* **1992**, 1933–1936.

Scheme 3. Calculated Fragmentation Pathways for Precursor **1**[a]

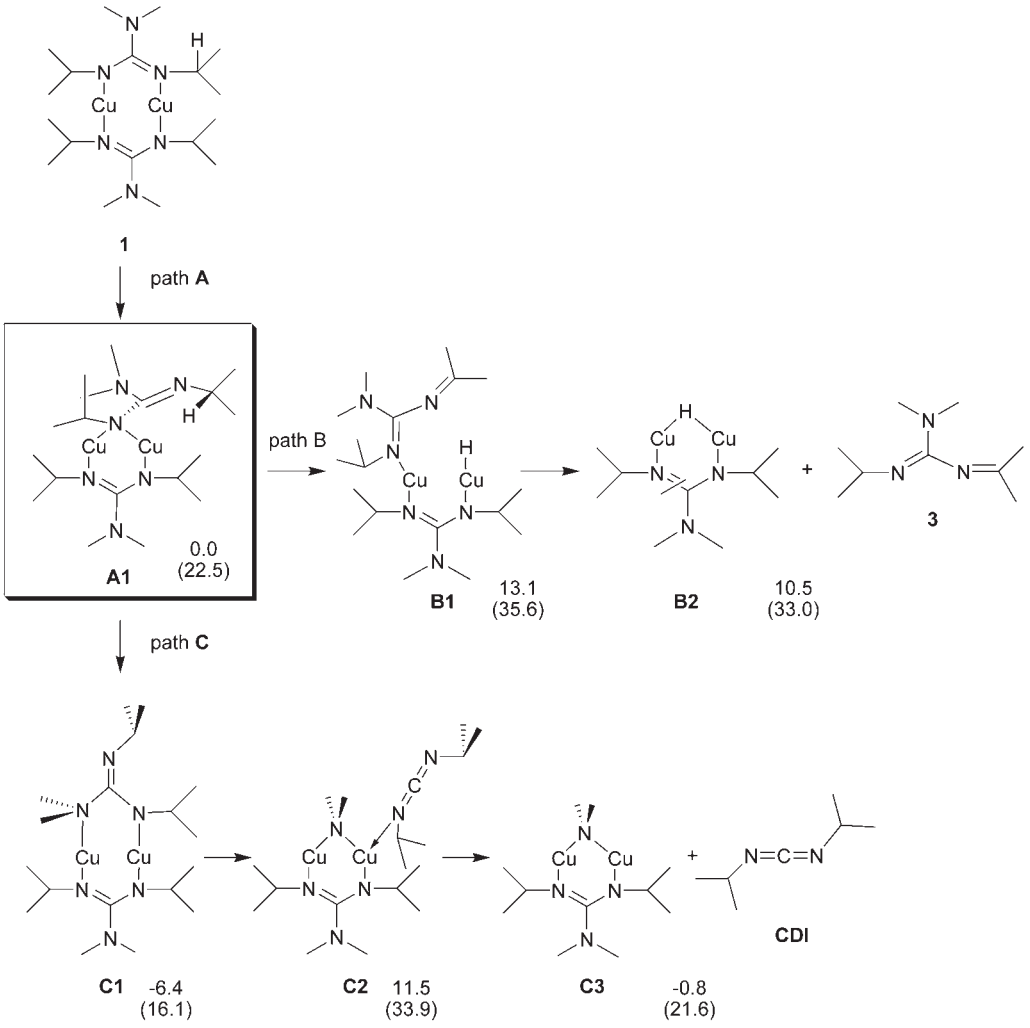

[a] Free energies relative to **A1** for the reaction steps are shown (values in parentheses are relative to species **1**).

(BLYP/6-31G(d))[24]/experimental frequencies for ν(C6═N1) were 1652.9/1668.9 and for ν(C1═N2) they were 1598.8/1635.1 cm^{-1} (Figure 4). The calculated intensity pattern (ca. 3:1) also fits well to the measured peak ratios: the two IR bands at lower frequencies are more intense than those at higher frequencies. However, these assignments are only tentative. For an unambiguous assignment of experimental IR bands, a complete vibrational analysis of **3** would be necessary. Such an analysis would necessarily be based on experimental IR data of different isotopomers of **3**, which would require extended synthetic work first. However, such an investigation is beyond the scope of our present work.

It is interesting that the thermolysis at these temperatures found no indication of CDI, as was previously found in sealed NMR tube thermolysis experiments.[11] An extensive DFT study of the decomposition of compound **1** was undertaken, and this helps rationalize these two different thermolysis pathways. These calculations were undertaken at the B3LYP/6-31+G(d,p) level of theory employing DCPs.

DFT Calculations. The calculated mechanism showed that **1** undergoes a shift of a nitrogen atom of one of the guanidinate ligands from an μ^1 to a μ^2 bonding arrangement, as well as a rotation of one of this ligand's isopropyl groups such that the hydrogen on this group is oriented toward one copper center (Scheme 3, path A). This step is calculated to be uphill in free energy by 22.5 kcal/mol. The resulting species **A1** is the branching point between β-hydrogen elimination (path B) and CDI elimination (path C).

As shown in path B of Scheme 3, compound **3** can be formed through elimination of the isopropyl methine proton to form a copper hydride (**B1**), which is an uphill process by 13.1 kcal/mol (free energy). The hydride **B1** eliminates **3** in a barrierless process. The path from **A1** to the products **B2** and **3** is endergonic by 10.5 kcal/mol (33.0 kcal/mol from **1**).

(24) Frisch, M. J.; Trucks, G. W.; Schlegel, H. B.; Scuseria, G. E.; Robb, M. A.; Cheeseman, J. R.; J. A. Montgomery, J.; Vreven, T.; Kudin, K. N.; Burant, J. C.; Millam, J. M.; Iyengar, S. S.; Tomasi, J.; Barone, V.; Mennucci, B.; Cossi, M.; Scalmani, G.; Rega, N.; Petersson, G. A.; Nakatsuji, H.; Hada, M.; Ehara, M.; Toyota, K.; Fukuda, R.; Hasegawa, J.; Ishida, M.; Nakajima, T.; Honda, Y.; Kitao, O.; Nakai, H.; Klene, M.; Li, X.; Knox, J. E.; Hratchian, H. P.; Cross, J. B.; Bakken, V.; Adamo, C.; Jaramillo, J.; Gomperts, R.; Stratmann, R. E.; Yazyev, O.; Austin, A. J.; Cammi, R.; Pomelli, C.; Ochterski, J. W.; Ayala, P. Y.; Morokuma, K.; Voth, G. A.; Salvador, P.; Dannenberg, J. J.; Zakrzewski, V. G.; Dapprich, S.; Daniels, A. D.; Strain, M. C.; Farkas, O.; Malick, D. K.; Rabuck, A. D.; Raghavachari, K.; Foresman, J. B.; Ortiz, J. V.; Cui, Q.; Baboul, A. G.; Clifford, S.; Cioslowski, J.; Stefanov, B. B.; Liu, G.; Liashenko, A.; Piskorz, P.; Komaromi, I.; Martin, R. L.; Fox, D. J.; Keith, T.; Al-Laham, M. A.; Peng, C. Y.; Nanayakkara, A.; Challacombe, M.; Gill, P. M. W.; Johnson, B.; Chen, W.; Wong, M. W.; Gonzalez, C.; Pople, J. A. *Gaussian 03*, Revision D.02 ed.; Gaussian, Inc.: Wallingford, CT, 2004.

Instead of undergoing β-hydrogen elimination, **A1** can undergo a shift of the nitrogen back to μ^1 coordination, with a concurrent rotation about the Cu−N bond to allow the exocyclic dimethylamido to coordinate to the other copper atom to form species **C1**. This step is thermodynamically downhill by 6.4 kcal/mol. Compound **C1** can then eliminate the dimethylamido moiety to give the copper compound **C2**, which further reacts to form **C3** and free CDI. Energetically, the process from **A1** to products **C3** and CDI is exergonic by 0.8 kcal/mol (but endergonic by 21.6 kcal/mol from **1**).

These calculations are a good model for the vapor phase decomposition, and show that β-hydrogen abstraction is the more thermodynamically favored for decomposition of **1** to metallic copper (as suggested in Scheme 2). However, the previously reported thermolysis to eliminate carbodiimide by deinsertion was performed at lower temperatures and in the solution phase.[11] These calculations also show that carbodiimide deinsertion is reasonable as a decomposition mechanism, as demonstrated by the convincing divergence at species **A1**.

Fragmentation at Higher Temperatures. We investigated the fragmentation of the copper precursor **1** and the protonated ligand **2** at temperatures of up to 800 °C, and new fragments appeared in the thermolyses of both **1** and **2**. Figure 5 shows the results of two series of thermolysis, spectrum A for **2** and spectrum B for **1**. As shown in Figure 5, the amount of species **3** (171.2 u), which is a key fragment of the thermolysis of precursor **1**, decreased with increasing temperature, while only two signals, at 124.1 and 45.0 u, showed a significant increase of intensity. The lower mass at 45.0 u fits to Me_2NH (calculated mass of 45.06 u) and the one at higher mass fits to the carbodiimide **4** (calculated mass of 124.10 u, Chart 2). These data indicate that the thermolysis product **3** eliminates Me_2NH to give the carbodiimide **4**. This interpretation is consistent with the decomposition of the protonated ligand **2** (Figure 5A). The signal for $\mathbf{2}^+$ dropped off, whereas signals at 126.1 and 45.0 u rose with increasing temperatures, showing that **2** eliminates Me_2NH to give the well-known CDI (Chart 2). As species **3** is also produced in the thermolysis of **2**, its signal at 171.2 u decreased (Figure 5). The intensity for the signal of CDI (126.1 u) varies over the temperature range but does not show a trend, which might be due to its overall low intensity.

The TOF MS data and their interpretation are consistent with MI FTIR data obtained from high temperature thermolyses. For example, in the thermolysis of **2** at 700 °C we unambiguously identified $HNMe_2$ and CDI, trapped in solid argon (Supporting Information, Figure S6). In the thermolysis of **1**, $HNMe_2$ was identified, but the unknown carbodiimide **4** could not be unambiguously identified, as a required IR spectrum for comparison is unknown in the literature. However, an intense and structured IR band with a maximum at 2127.7 cm^{-1} clearly indicates the presence of a carbodiimide. Moreover, an IR band in the typical range of C=C valence vibrations at 1649.2 cm^{-1} supports the proposed structure of **4** (see Chart 2). Frequency calculations on **4** at the BLYP/6-31G(d) level of theory give a C=C stretch at 1639.0 cm^{-1} and a N=C=N asymmetric stretch at 2164.7 cm^{-1}.

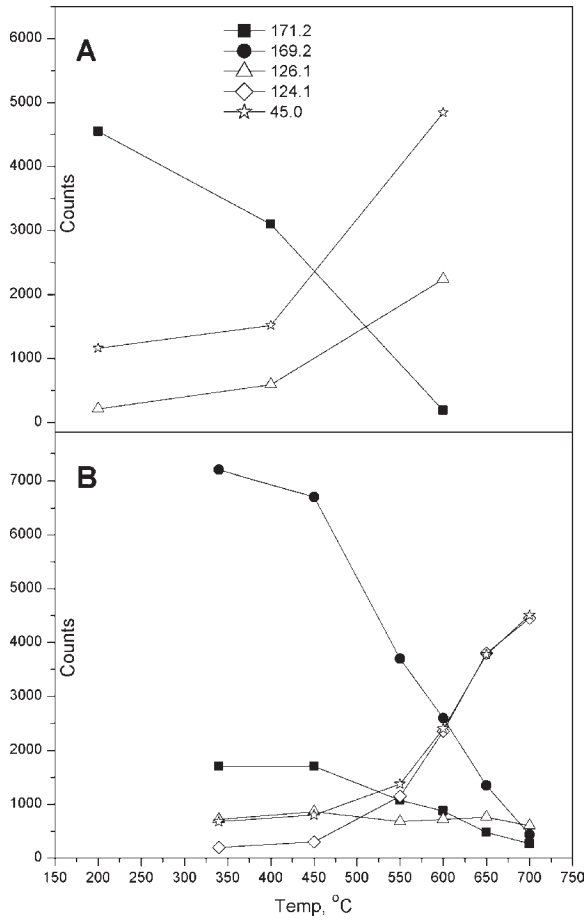

Figure 5. Temperature dependences of selected ions of the thermolysis at high temperatures of **1** (spectrum B) and **2** (spectrum A) [m/z = 171.2 ($\mathbf{2}^+$), 169.2 ($\mathbf{3}^+$), 126.2 ($\mathbf{4}^+$), 124.1 (**CDI**$^+$) 45.0 ($HNMe_2^+$) u]. The intensities of masses at 169.2 and 124.1 u were negligible in spectrum A (counts between 2 and 22 at sweep rates of 8×10^6).

Chart 2. Carbodiimides

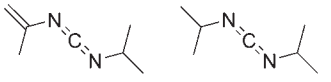

4 (124.10 u) **CDI** (126.12 u)

Summary and Conclusions

The fragmentation of the dimeric copper(I) precursor $[Me_2NC(NiPr)_2Cu]_2$ (**1**) has been investigated with TOF MS, MI FTIR spectroscopy, and DFT calculations. The experimental results showed that precursor **1** fragments above oven temperatures of 150 °C to release the oxidized guanidine $Me_2NC(=NiPr)(N=CMe_2)$ (**3**). In addition to **3**, the formation of H_2 was detected by TOF MS. The key intermediate **3** was synthesized independently in this study and through comparison of FTIR spectra of matrix-isolated **3** with those from thermolysis experiment with copper precursor **1**, the formation of the oxidized guanidine **3** as a product of the thermolysis was proven. The structure of the major IR bands could be rationalized with the help of DFT calculations, which showed that species **3** exists as a predomination of the *trans* isomer. These findings can be explained by assuming a β-hydrogen elimination of the ligands in precursor **1** takes place. DFT calculations indicated that the two decomposition mechanisms result from the same parent species (**A1**), which rationalizes the fact that carbodiimide deinsertion is seen at lower temperatures in the

solution phase, but β-hydrogen elimination is favored in higher temperature, gas-phase reactions.

When higher temperatures were explored, it became evident that both species **2** and species **3** underwent deinsertion to form free amine and either CDI or **4**, respectively. This important observation indicates that CDI detected at high temperatures can result from deinsertion from a thermolysis product, and not necessarily from the precursor itself.

Experimental Section

General Remarks. Complex **1** was synthesized via known procedures[11] and purified by sublimation prior to use (**1**: 70−77 °C, approximately $10^{-2}-10^{-3}$ mbar). Compound **2** and was synthesized via known procedures[22] and purified via flask-to-flask condensation at ambient temperatures (approximately $10^{-2}-10^{-3}$ mbar).

The matrix isolation and the TOF MS apparatus were separate instruments each equipped with its own thermolysis oven, both identical in construction. Both instruments used the same carrier gas supply and were in close proximity so that the heatable container, loaded with the compound of interest, could be moved from one to the other instrument without exposing the sample to air. Both instruments used the same thermolysis oven temperature controller. The facility was constructed in this way so that a series of experiments with one sample batch could be performed using one method, for example, MI FTIR spectroscopy, followed by a series of experiments using the other method, for example, TOF MS, and still being able to keep the experimental conditions similar in both consecutive series of experiments.

Each thermolysis oven was equipped with an Al_2O_3 tube (OD = 4 mm) with two parallel, inner canals (ID = 1 mm). The overall length of the Al_2O_3 tube was 35 mm with the last 10 mm heated with a tungsten wire, coiled around the outside, and coated with ZrO_2 cement. One of the inner canals was equipped with a thermocouple (Thermocoax: NiCrSi/NiSi), while the second canal was used to let a carrier gas/sample mixture pass through. With this setup, reliable thermolysis temperatures at the inside of the thermolysis tube could be measured without exposing the thermocouple to the gaseous sample. A schematic drawing of the thermolysis oven can be found in reference 26.

A thermolysis series with compound **1** was done in the temperature range between 100 and 800 °C for both MI FTIR spectroscopy and TOF MS. The thermolysis of compound **2** was investigated in the temperatures range 200 to 800 °C for both MI FTIR spectroscopy and TOF MS.

MI FTIR Spectroscopy. The matrix apparatus consisted of a vacuum line (Varian TV 551 Navigator; Varian DS 402) and a Sumitomo CSW-71 cryogenic closed cycle system (Sumitomo Heavy Industries. Ltd.) including a Sumitomo RDK-415D 4K cold head fitted with CsI windows (vacuum shroud design and fabrication by Janis Research Company, Inc.). The sample was loaded into a heatable container connected to the thermolysis oven. In a typical experiment, the evacuated container, loaded with the compound of interest, was kept at constant temperature (**1**: 86 °C; **2**: 0 °C) while a flow of argon (1.25 sccm; Praxair 6.0) was conducted over the sample (mass-flow controller: MKS Type 1179A). The resulting gaseous mixture was passed through a thermolysis oven for 30−90 min and deposited onto a CsI window cooled to 20 K. The distance between the end of the heated oven tube and the CsI window was 54 mm. The so-prepared matrixes were cooled to 4 K for FTIR measurements (Bruker Tensor 27 FTIR; 200 to 5000 cm^{-1}; resolution of 1 cm^{-1}).

TOF MS. The apparatus consisted of a custom designed vacuum chamber (designed by Stefan Kaesdorf, Geräte für Forschung and Industrie; built by Johnsen Ultravac Inc.), equipped with one roughing vacuum pump (Varian DS 602) and three turbo vacuum pumps, and a reflectron TOF spectrometer with electron impact ionization (Stefan Kaesdorf, Geräte für Forschung and Industrie; time resolution under favorable conditions $T/\Delta T = 10000$). For more details please see reference 12 (Note that the distance between the end of the heated oven tube to the orifice of the skimmer was shortened from 12 to 8 mm.). In a typical experiment, the sample container was kept at constant temperature (**1**: 90−92 °C; **2**: 0 °C) while a flow of argon was conducted over the sample. To get acceptable signal-to-noise ratios, the container temperature for **1** needed for the TOF MS measurements was slightly higher than those for MI FTIR spectroscopy (see above). For all measurements electron impact of 70 eV and 1 to 20 million sweeps per oven temperature were applied. The signal of the carrier gas argon at 40 u was reduced in intensity by using a mass filter at 4.35 kV (delay: 3.1000 μs; duration: 0.9000 μs). This prevented the MCP detector from exceeding its detection limit. Calibration of flight times was done within every new series of measurements using Xe as an additional standard. Calibrations were done with the following masses: $^{129}Xe^+$ (128.90478 u), $^{129}Xe^{2+}$ (64.45239 u), $^{40}Ar^+$ (39.96230 u), and $H_2{}^{16}O^+$ (18.01056 u). As the calibration masses did not span the entire range of measured ions from **1**, the experimental masses were usually within the range of ±0.1 u of the calculated ones.

Calculated masses of selected ions (intensities in parentheses): $\mathbf{1}^+$ ($C_{18}H_{40}Cu_2N_6^+$): m/z = 466.19 (100.0%), 467.19 (19.5%), 467.19 (2.2%), 468.19 (89.1%), 468.20 (1.8%), 469.19 (17.4%), 469.19 (2.0%), 470.19 (19.9%), 470.20 (1.6%), 471.19 (3.9%).

DFT Calculations. All calculations were done using the GAUSSIAN 03 program package.[24,25] The mechanism[25,26] of thermolysis of **1** was studied with the B3[27]LYP[28] functional and the 6-31+G(d,p) basis set augmented with dispersion correcting potentials (DCPs).[29] DCPs are atom-centered effective core potentials which are employed to better account for long-range dynamical correlation effects (i.e., dispersion interactions). Coefficients for DCPs have been optimized[30] for a wide variety of functionals and basis sets and can be implemented into quantum chemical software simply by appending the input file. All thermodynamic values discussed in the text are calculated free energies at 260 °C. To help interpret the IR spectra acquired, molecular vibrations were studied at the BLYP/6-31G(d) level of theory. The BLYP functional was used rather than B3LYP as it is known that unscaled frequencies obtained from BLYP are more accurate than those from B3LYP.[31]

Acknowledgment. We thank the Natural Sciences and Engineering Research Council of Canada (NSERC Discovery Grants, J.M. and S.T.B.) for their generous support. We thank the Canada Foundation for Innovation (CFI) and the government of Saskatchewan for funding of the MI FTIR spectrometer and the TOF MS facility.

Supporting Information Available: FTIR spectra of matrix-isolated species **1**, **2**, and **3**, and FTIR spectra of thermolysis of **1** and **2** (Figures S1−S6; range 4000−220 cm^{-1}); Cartesian coordinates for the *trans*-**3** species, as well as the species in Figure 4 (Tables S1−S11). This material is available free of charge via the Internet at http://pubs.acs.org.

(25) Farrugia, L. J. *J. Appl. Crystallogr.* **1997**, *30*, 565.
(26) Müller, J.; Wittig, B.; Sternkicker, H.; Bendix, S. *J. Phys. IV* **2001**, *11*, 17–22.
(27) Becke, A. D. *J. Chem. Phys.* **1993**, *98*, 5648–5652.
(28) Lee, C.; Yang, W.; Parr, R. G. *Phys. Rev. B* **1988**, *37*, 785–789.
(29) DiLabio, G. A. *Chem. Phys. Lett.* **2008**, *455*, 348–353.
(30) Mackie, I. D.; DiLabio, G. A. *J. Phys. Chem. A* **2008**, *112*, 10968–10976.
(31) Rauhut, G.; Pulay, P. *J. Phys. Chem.* **1995**, *99*, 3093–3100.